

## SI-Decoding the Influence of Monomer Structures on the Electrical Double-Layer of Alkaline Fuel Cells

Xiao-Hui Yang,<sup>†,‡</sup> Lin Zhuang,<sup>¶</sup> and Jun Cheng\*,<sup>†,§,‡</sup>

<sup>†</sup>State Key Laboratory of Physical Chemistry of Solid Surfaces, iChEM, College of  
Chemistry and Chemical Engineering, Xiamen University, Xiamen 361005, China

<sup>‡</sup>National Engineering Research Center of High-end Electronic Chemicals (Reconstructed),  
Xiamen University, Xiamen 361005, China

<sup>¶</sup>College of Chemistry and Molecular Sciences, Hubei Key Lab of Electrochemical Power  
Sources, Wuhan University, Wuhan 430072, China

<sup>§</sup>Innovation Laboratory for Sciences and Technologies of Energy Materials of Fujian  
Province (IKKEM), Xiamen, China

E-mail: [chengjun@xmu.edu.cn](mailto:chengjun@xmu.edu.cn)

### Computational methods

- 1. Force field parameters.** The initial all-atomic MD simulations were constructed using Moltemplate<sup>1</sup> and Packmol<sup>2</sup> packages, and carried out using the Lammmps package. We employed conventional parameters inherited from OPLS/AA to describe the QAPS and QAPPT polymer, and used the SPC/E water model to reproduce the aqueous environment. The restrained electrostatic potential (RESP) approach was used to assign partial charges of the QAPS and QAPPT. The RESP charges are generated as follows: First, all molecules were optimised in B3LYP/6-311g(d,p) DFT level using Gaussian 16 software,<sup>3</sup> where the solvation effect is corrected using the PCM method for the aqueous environment.<sup>4</sup> Then, the RESP charges are mixed as a protocol of 60% aqueous and 40% gas-phase charges.<sup>5</sup> The Lennard-Jones parameters for OH<sup>-</sup> anion were adopted from Bonthuis *et al.*'s work<sup>6</sup>, and for the graphene electrode was adopted from Werder *et al.*'s work.<sup>7</sup> The geometric mixing rule is applied in this work to have good compatibility with the OPLS/AA force field.
- 2. Simulation details.** Each graphene electrode was 51.13 x 49.2 Å and made of 2880 carbon atoms arranged in 3 layers of 960 atoms each. 2D periodic boundary conditions (PBC) were

used in the xy directions. The simulations were first performed in the NPT ensemble in the 2D-PBC model at 330K and 1 bar. To implement the NPT ensemble in a 2D model, we apply a specific force ( $F=0.0367$  kcal/(mol·Å) in this work) on both ends of the z-direction (*i.e.*, electrodes), and then make the pressure generated by this force on the electrode surface equal to the pressure of 1 bar. The electrodes are neutral at this stage, corresponding to the potential of zero charge (PZC) in electrochemistry. The SHAKE algorithm was employed to constrain the stretching mode involving hydrogen atoms, and thus the timestep can be 1 fs. This pre-equilibrium period takes at least 150 ns until the potential in the middle of the electrolyte (bulk region) is horizontal, and the potential profiles near the electrodes at both ends are symmetrical. Then we adjust the electrode potential by using the USER-CONP2 package. Fixed cell voltages between two planar graphene electrodes were applied. After ca. 50 ns pre-equilibrium, the potential in the bulk region of the electrolyte is horizontal. At last, we ran a 10 ns production period and aligned the potential in the bulk region of the electrolyte with the PZC result (Figure S1), and obtained the density profile of each interface. For the graphite/QAPS system, the density of the bulk region is also checked among all trajectories, and the variation is less than 2% (of each molecule, the variation is less than 10%). In comparison, the graphite/QAPPT system has a maximum variation of the bulk region of 3%, while for each component, the variation is less than 5%.

- 3. Validation of the force field.** To verify the suitability of the OPLS-AA force field in capturing  $\pi$ - $\pi$  interactions, we calculated the adsorption energy of a benzene molecule on a graphene surface at various tilt angles using both OPLS-AA and DFT (vdW-DF functional) methods. As shown in Figure S3, the adsorption energy profile obtained from OPLS-AA agrees well with quantum chemical results in both trend and magnitude, supporting the reliability of our force field in modeling aromatic stacking interactions.
- 4. Effect of hydration level on EDL structure.** To evaluate the influence of hydration degree on the interfacial electric double layer (EDL), we performed additional CMD simulations at different water contents ( $\lambda = 20, 60$ ). As shown in Figure S4, the density profiles of the ionomer near the electrode remain qualitatively consistent across hydration levels, confirming that the main trends reported in the main text are robust to hydration variation.
- 5. CMD simulation error.** The applied potential in our simulations (e.g., -3.4 V vs. PZC) exceeds

the typical electrochemical window used in practical fuel cell applications. We would like to clarify our rationale in the following points:

- a) Although the applied potential appears large, our classical force field model underestimates the double-layer capacitance compared to experimental systems, as also discussed in our response to Comment 3. This underestimation results in a reduced surface charge density and a correspondingly weaker interfacial electrostatic field. As noted in *J. Chem. Phys.* 2023, 158, 084701, simulations employing classical force fields typically require higher potentials to achieve comparable electrostatic responses. Based on this consideration, we estimate that the interfacial electrostatic strength at  $-3.4$  V vs. PZC in our simulations is equivalent to approximately  $-1.6$  V vs. PZC in realistic systems.
- b) At this potential regime, despite being close to the onset of faradaic processes in real electrochemical systems, the interfacial double-layer structure remains physically relevant. The use of enhanced field strength helps to amplify molecular-level differences (e.g., between rigid and flexible polymers), allowing us to better resolve the structural response under otherwise subtle conditions.
- c) As our study is based on classical molecular dynamics, the simulation framework does not explicitly represent electrons and cannot capture faradaic processes such as hydrogen evolution or carbon corrosion. Therefore, while our applied potentials are beyond the electrochemical window, no undesired electrochemical side reactions occur in the simulation. Nevertheless, we acknowledge that such reactions may emerge in real electrochemical systems and that their impact on long-term interface stability is an important direction for future quantum-based investigations.

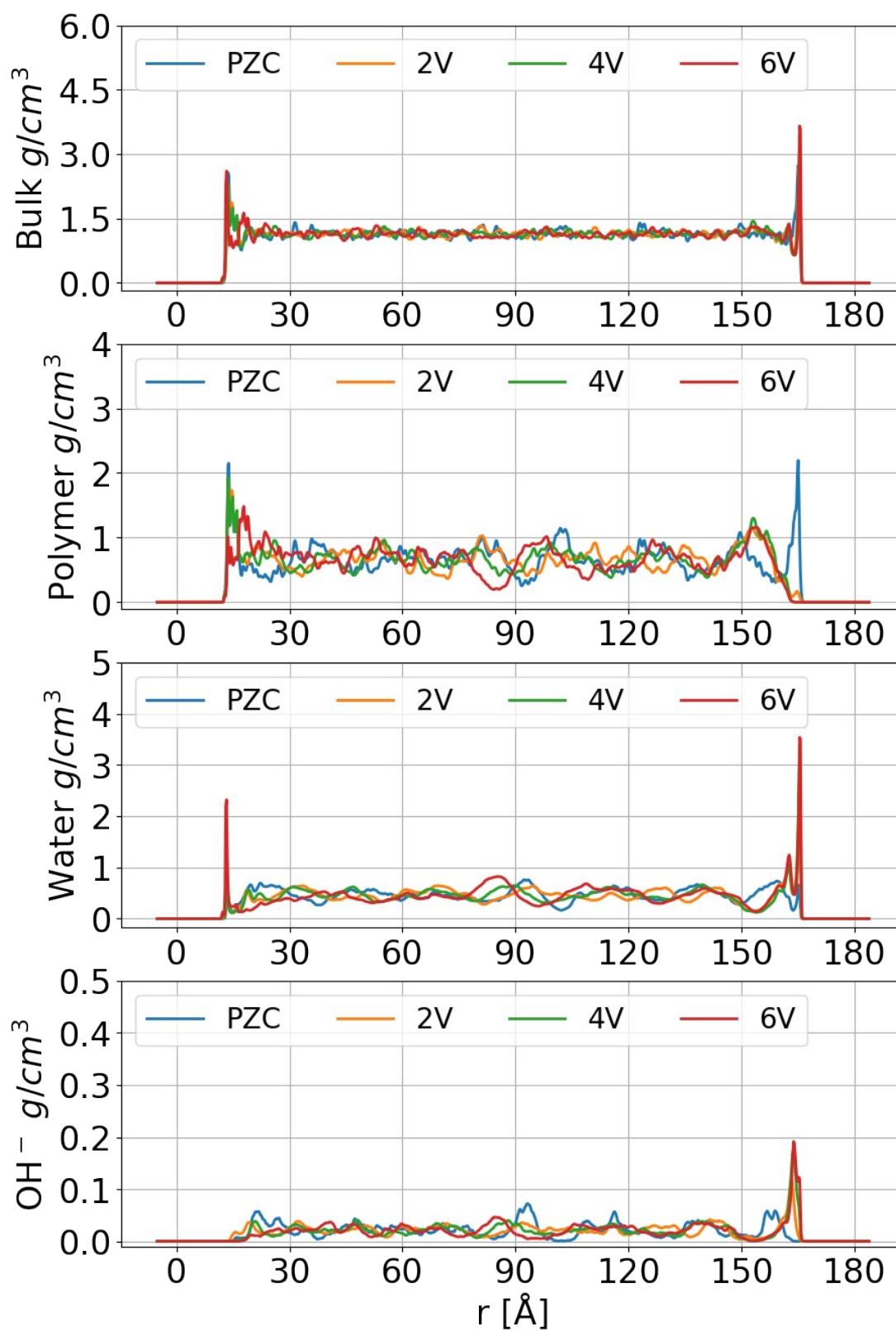


Figure S1. Density profiles of graphene/QAPS full cell simulations at different electrode potentials.

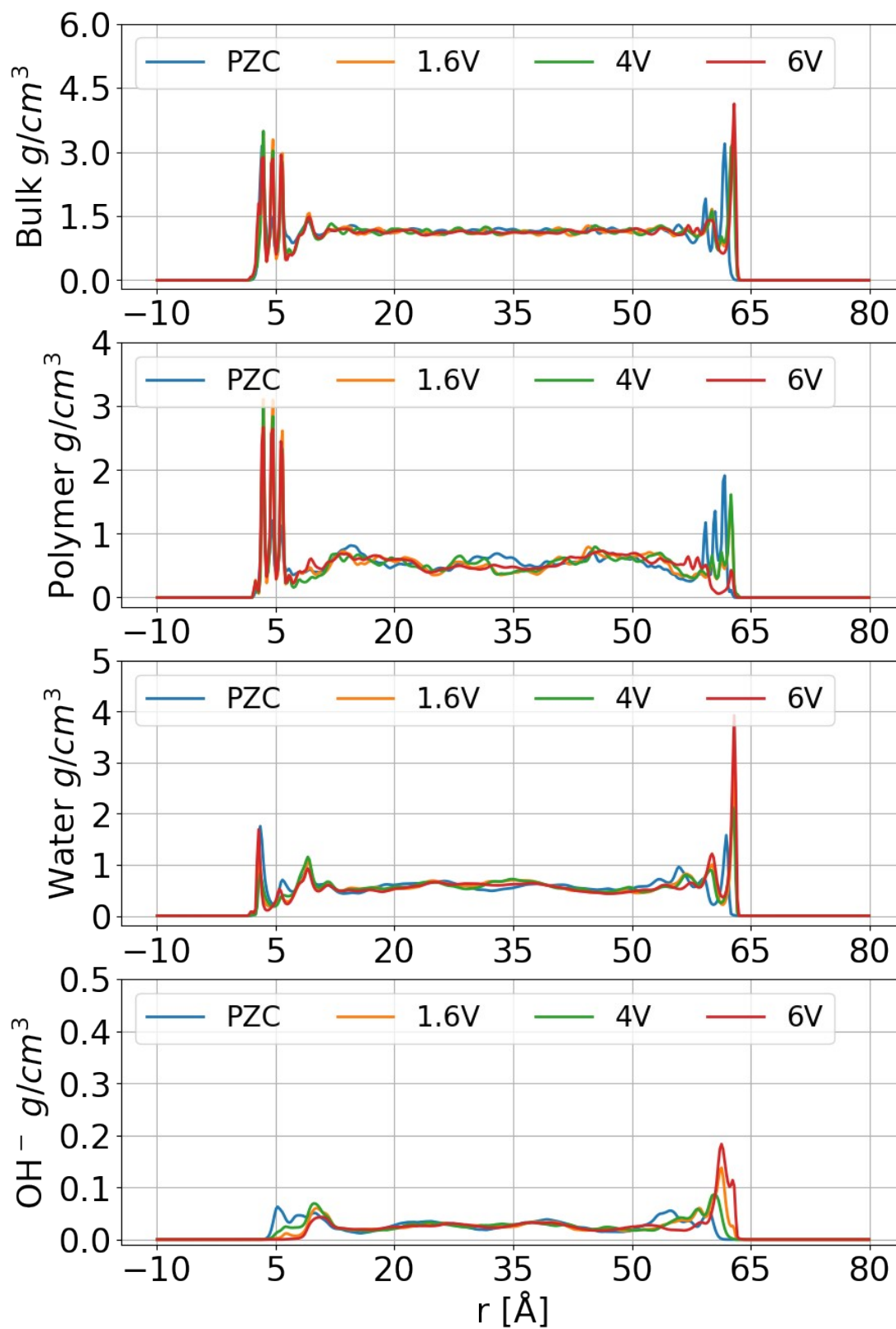


Figure S2. Density profiles of graphene/QAPPT full cell simulations at different electrode potentials.

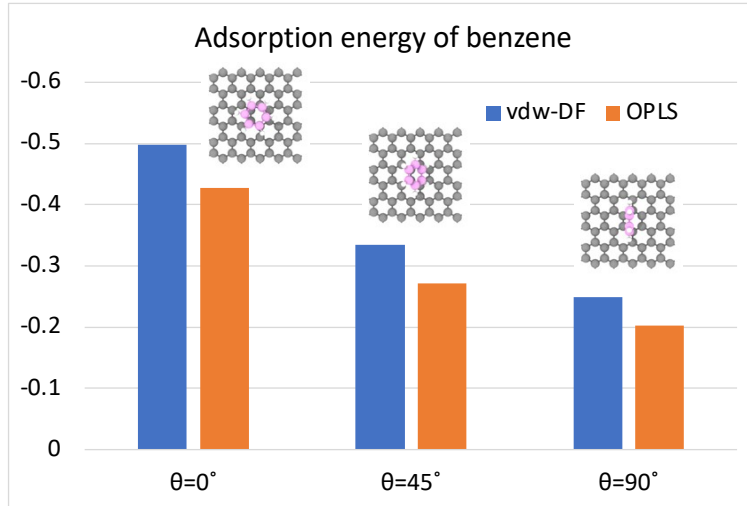


Figure S3. Adsorption energy (in eV) of benzene on a graphene surface.  $\theta$  denotes the angle between the benzene ring and the graphene surface.

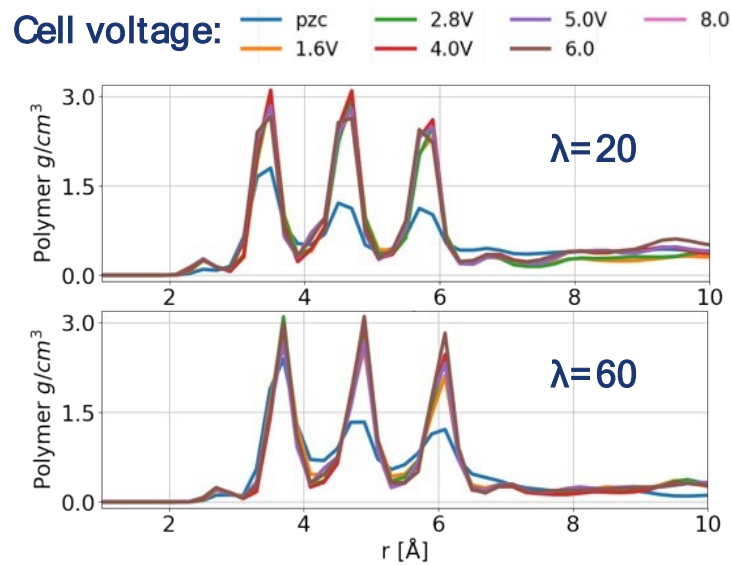


Figure S4. Density profiles of the QAPPT ionomer at graphene-polyelectrolyte interfaces under different cell voltage and hydration conditions.

## Reference

(1) Jewett, A. I.; Stelter, D.; Lambert, J.; Saladi, S. M.; Roscioni, O. M.; Ricci, M.; Autin, L.; Maritan, M.; Bashusqeh, S. M.; Keyes, T.; Dame, R. T.; Shea, J.-E.; Jensen, G. J.; Goodsell, D. S. Moltemplate: A Tool for Coarse-Grained Modeling of Complex Biological Matter and

Soft Condensed Matter Physics. *J. Mol. Biol.* **2021**, *433* (11), 166841. <https://doi.org/10.1016/j.jmb.2021.166841>.

(2) Martínez, L.; Andrade, R.; Birgin, E. G.; Martínez, J. M. PACKMOL: A Package for Building Initial Configurations for Molecular Dynamics Simulations. *J. Comput. Chem.* **2009**, *30* (13), 2157–2164. <https://doi.org/10.1002/jcc.21224>.

(3) Gaussian 16, Revision A.03, M. J. Frisch, G. W. Trucks, H. B. Schlegel, G. E. Scuseria, M. A. Robb, J. R. Cheeseman, G. Scalmani, V. Barone, G. A. Petersson, H. Nakatsuji, X. Li, M. Caricato, A. V. Marenich, J. Bloino, B. G. Janesko, R. Gomperts, B. Mennucci, H. P. Hratchian, J. V. Ortiz, A. F. Izmaylov, J. L. Sonnenberg, D. Williams-Young, F. Ding, F. Lipparini, F. Egidi, J. Goings, B. Peng, A. Petrone, T. Henderson, D. Ranasinghe, V. G. Zakrzewski, J. Gao, N. Rega, G. Zheng, W. Liang, M. Hada, M. Ehara, K. Toyota, R. Fukuda, J. Hasegawa, M. Ishida, T. Nakajima, Y. Honda, O. Kitao, H. Nakai, T. Vreven, K. Throssell, J. A. Montgomery, Jr., J. E. Peralta, F. Ogliaro, M. J. Bearpark, J. J. Heyd, E. N. Brothers, K. N. Kudin, V. N. Staroverov, T. A. Keith, R. Kobayashi, J. Normand, K. Raghavachari, A. P. Rendell, J. C. Burant, S. S. Iyengar, J. Tomasi, M. Cossi, J. M. Millam, M. Klene, C. Adamo, R. Cammi, J. W. Ochterski, R. L. Martin, K. Morokuma, O. Farkas, J. B. Foresman, and D. J. Fox, Gaussian, Inc., Wallingford CT, 2016.

(4) Miertuš, S.; Scrocco, E.; Tomasi, *J. Chem. Phys.*, **1981**, *55*, 117-129

(5) Schauerl, M.; Nerenberg, P. S.; Jang, H.; Wang, L.-P.; Bayly, C. I.; Mobley, D. L.; Gilson, M. K. Non-Bonded Force Field Model with Advanced Restrained Electrostatic Potential Charges (RESP2). *Commun Chem* **2020**, *3* (1), 44. <https://doi.org/10.1038/s42004-020-0291-4>.

(6) Bonthuis, D. J.; Mamatkulov, S. I.; Netz, R. R. Optimization of Classical Nonpolarizable Force Fields for OH<sup>-</sup> and H<sub>3</sub>O<sup>+</sup>. *J Chem Phys* **2016**, *144* (10), 104503. <https://doi.org/10.1063/1.4942771>.

(7) Werder, T.; Walther, J. H.; Jaffe, R. L.; Halicioglu, T.; Koumoutsakos, P. On the Water–Carbon Interaction for Use in Molecular Dynamics Simulations of Graphite and Carbon Nanotubes. *J Phys Chem B* **2003**, *107* (6), 1345–1352. <https://doi.org/10.1021/jp0268112>.